The Photosensitizing Clinical Agent Verteporfin is an Inhibitor of SPAK and OSR1 Kinases

Mubarak A. AlAmri,[b] Hachemi Kadri,[a] Luke J. Alderwick,[c] Mark Jeeves,[d] Youcef Mehellou,*[a]

Abstract: SPAK and OSR1 are two serine/threonine protein kinases that play important key roles in regulating ion homeostasis. Various SPAK and OSR1 mouse models exhibited reduced blood pressure. Herein, we report the discovery of Verteporfin, a photosensitizing agent used in photodynamic therapy, as a potent inhibitor of SPAK and OSR1 kinases. We show that Verteporfin binds the kinase domains of SPAK and OSR1 and inhibit their catalytic activity in an ATP-independent manner. In cells, Verteporfin was able to suppress the phosphorylation of the ion co-transporter NKCC1, a downstream physiological substrate of SPAK and OSR1 kinases. Kinase panel screening indicated that Verteporfin inhibited a further eight protein kinases more potently than SPAK and OSR1. Although Verteporfin has largely been studied as a modifier of the Hippo signaling pathway, this work indicates that the WNK-SPAK/OSR1 signaling cascade is also a target of this clinical agent. This finding could explain the fluctuation in blood pressure noted in patients and animals treated with this drug.

Introduction

The STE20/SPS1-related proline/alanine-rich kinase (SPAK) and the oxidative-stress-responsive kinase 1 (OSR1) are two closely related serine/threonine protein kinases that play essential roles in regulating ion homeostasis and blood pressure.[1] SPAK and OSR1 kinases are 68% identical in sequence and share a 92-amino acids highly conserved carboxy-terminal (CCT) domains (aa. 436-527 for OSR1 and 456-547 for SPAK), which are themselves 79% identical in sequence.[2] They are activated by osmotic stress or hypotonic (low chloride) environments resulting in phosphorylation at their T-loops by a family of protein kinases known as with no lysine (WNK) kinases 1-4 (**Figure 1A**).[3] Upon WNK activation, SPAK and OSR1 kinases bind to the scaffolding protein Mouse Only protein 25 (MO25),[4] of which in humans two isoforms α and β are expressed, resulting in a further 80- to 100-fold increase in their in vitro kinase activity (**Figure 1A**).[5] Subsequently, SPAK and OSR1 kinases in complex with MO25 phosphorylate an array of ion co-transporters such as the Na^+-K^+-Cl^- co-transporters 1 and 2 (NKCC1 and 2), the Na^+-Cl- co-transporter (NCC) and K^+-Cl^- co-transporter (KCC), which are the molecular targets of the antihypertensive loop and thiazide diuretics (**Figure 1A**).[1]

As genetic mutations in the WNK protein kinases, which regulate the function of SPAK and OSR1, cause an inherited form of hypertension in humans known as Gordon's syndrome,[6] SPAK and OSR1 have consequently been implicated in the regulation of blood pressure in humans.[7] The link between SPAK and OSR1 kinases and blood pressure was further strengthened by the discovery that the two E3 ubiquitin ligases, Cullin3 and KLHL3, which regulate the expression levels of WNK kinases,[8] are also mutated in some humans with an inherited form of hypertension[9]. To provide an in vivo evidence of the direct involvement of SPAK and OSR1 kinases in regulating blood pressure, numerous SPAK knock-in and knock-out mouse models were generated and these exhibited a reduction in blood pressure.[7] Such finding has stimulated interest in the discovery of new compounds that inhibit WNK, SPAK and OSR1 kinases and offer advantageous antihypertensive effects. To date, only few compounds that inhibit these kinases have been reported,[10] with the most promising and potent inhibitors being of WNK kinases[11] instead of SPAK and OSR1. Nevertheless, a selection of small molecules such as STOCK506099, Closantel and Rafoxanide have been reported as SPAK and OSR1 kinase inhibitors with moderate potency in vitro (**Figure 1B**).[12] These inhibitors could be divided into two groups; non-ATP competitive inhibitors and protein-protein interaction inhibitors. The first group of inhibitors, which includes STOCK1S-50699 and STOCK2S-26016, bind SPAK and OSR1 CCT domains and prevent their binding to the upstream WNK kinases and hence inhibiting their activation.[12a] The second group includes STOCK1S-14279, Closantel and Rafoxanide, which inhibit SPAK and OSR1 activity by binding to an allosteric site on their CCT domains and do not seem to interfere with the binding to WNK kinases.[12b, 12c]

Encouraged by the amenability of targeting and inhibiting SPAK and OSR1 kinases by small molecules and the potential of these inhibitors as antihypertensive agents, we embarked on discovering novel SPAK and OSR1 kinase inhibitors using a high-throughput screening (HTS) approach.

[a] Dr. Hachemi Kadri and Dr. Youcef Mehellou
School of Pharmacy and Pharmaceutical Sciences
Cardiff University
King Edward VII Avenue, Cardiff CF10 3NB (UK).
E-mail: MehellouY1@cardiff.ac.uk
[b] Mubarak A. AlAmri
School of Pharmacy
University of Birmingham
Edgbaston, Birmingham B15 2TT (UK).
[c] Dr. Luke J. Alderwick
School of Biosciences
University of Birmingham
Edgbaston, Birmingham B15 2TT (UK).
[d] Dr. Mark Jeeves
School of Cancer Sciences
University of Birmingham
Edgbaston, Birmingham B15 2TT (UK).

Supporting information for this article is given at the end of the document.

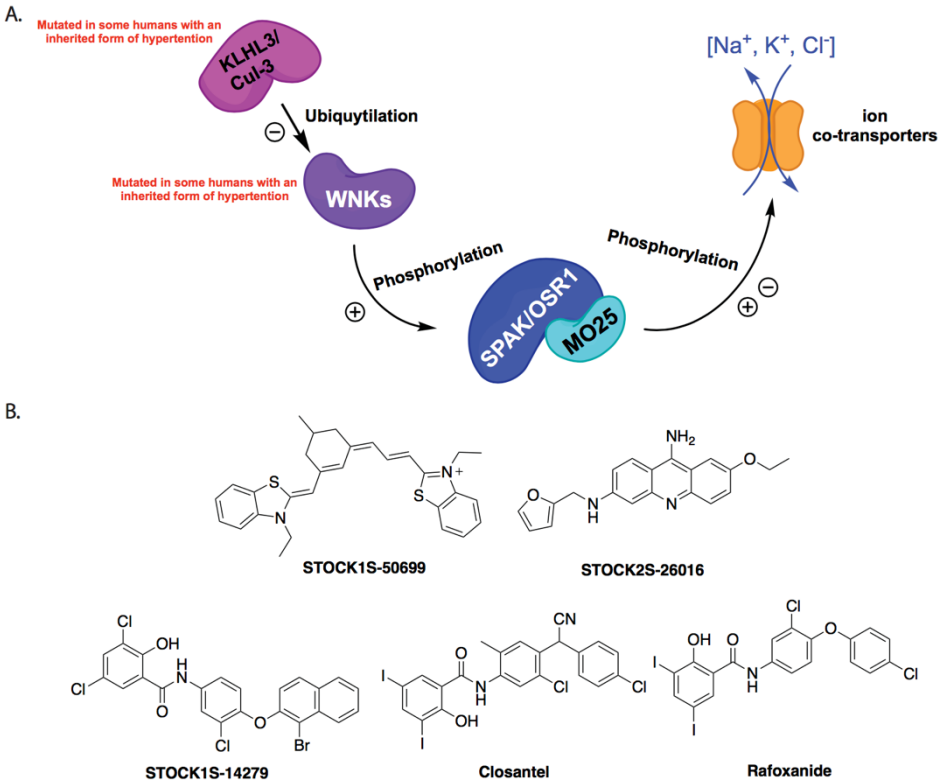

Figure 1. A summary of WNK-SPAK/OSR1 signaling cascade and the various reported SPAK and OSR1 kinase inhibitors. (**A**) WNK kinases, which are mutated in some humans with an inherited form of hypertension, become activated under osmotic stress and phosphorylate SPAK and OSR1 kinases. These subsequently bind the scaffolding protein MO25 and phosphorylate a selection of sodium, potassium and chloride ion co-transporters leading either to their activation or inhibition. (**B**) Chemical structures of reported compounds that inhibit SPAK and OSR1 kinases by binding to their *C*-terminal domain and either acting as allosteric inhibitors (Closantel, STOCK1S-14279 and Rafoxanide) or inhibitors of SPAK and OSR1 binding to their upstream WNK kinases (STOCK1S-50699 and STOCK2S-26016).

Results

Optimization of OSR1 HTS assay.

Most of the reported studies into the in vitro SPAK and OSR1 kinase activity employ radioactive ATP,[2, 5, 13] so we first had to develop and optimize a non-radioactive in vitro SPAK or OSR1 kinase assay compatible with HTS technologies. For this, we used Promega's ADP-Glo™ kinase assay,[14] which employs a luminescent ADP detection system instead of radioactive ATP. We previously used this assay for determining SPAK and OSR1 kinase activity in vitro though it was not optimized for HTS screening at that stage.[12c] For our HTS kinase assay, we decided to use *E.coli*-expressed full length human OSR1 T185E (1-527) (**Supplementary Figure S1**), where threonine 185 was mutated into glutamic acid to mimic WNK phosphorylation at this site, making the kinase constitutively active in vitro as previously reported (**Supplementary Figure S2**).[15] The choice of OSR1 T185E instead of SPAK T233E was due to the superior in vitro kinase activity exhibited by OSR1 T185E compared to SPAK T233E.[5, 15] As an in vitro OSR1 T185E substrate, we decided to use a fragment of the bacterially expressed human NKCC2 (1–174) encompassing the *N*-terminal cytoplasmic domain. This is readily obtained from *E.coli* expression systems (**Supplementary Figure S3**) and it was shown previously to be phosphorylated by OSR1 T185E in vitro at various threonine residues, precisely T95 and T100.[16] The optimal conditions for the 384-well plate HTS-compatible in vitro kinase assay were 0.2 μM OSR1 T185E, 5 μM human NKCC2 (1–174) (used as substrate), 0.1 mM ATP and 10 mM $MgCl_2$. These conditions gave an assay with a z' factor of 0.78 (minimum ≥ 0.5), signal-to-noise ratio (S/N) and signal-to-background ratio (S/B) were 94.6 (minimum > 10) and 16.9 (minimum > 3), respectively, indicating the robustness of our assay (**Supplementary Figure S4**).[17] Post-screening, the z' factor, signal window (SW), and coefficient of variation (CV) of each plate were calculated and compared with the minimum pass criteria to evaluate the quality of screening data. All parameters exceeded the minimum pass limits (see Experimental Section).[17]

Screening library of 1,200 compounds

Once the assay was optimized, we screened an in-house library of 1,200 FDA-approved compounds at a single concentration of 20 μM. This primary screen led to the identification of eighteen hits that achieved ≥ 40% inhibition of OSR1 T185E kinase activity in vitro (**Figure 2A**). To verify these initial hits, they were subsequently screened at 10 and 50 μM (**Figure 2B**). Only seven out of the initial eighteen hits were then found to inhibit OSR1 T185E in vitro in a dose-dependent manner giving an overall hit rate from this HTS exercise of 0.58%. Subsequently, the IC_{50} values of the seven verified hit compounds were determined using two different OSR1 T185E substrates, the bacterially expressed human NKCC2 (1-174) fragment, which we used in the HTS assay and an 18-mer peptide termed CATCHtide[2] that had been developed previously as a SPAK and OSR1 peptide substrate (**Figure 2C**). Verteporfin (**Figure 2D**), a benzoporphyrin derivative approved for use as a photosensitizer in photodynamic therapy,[18]

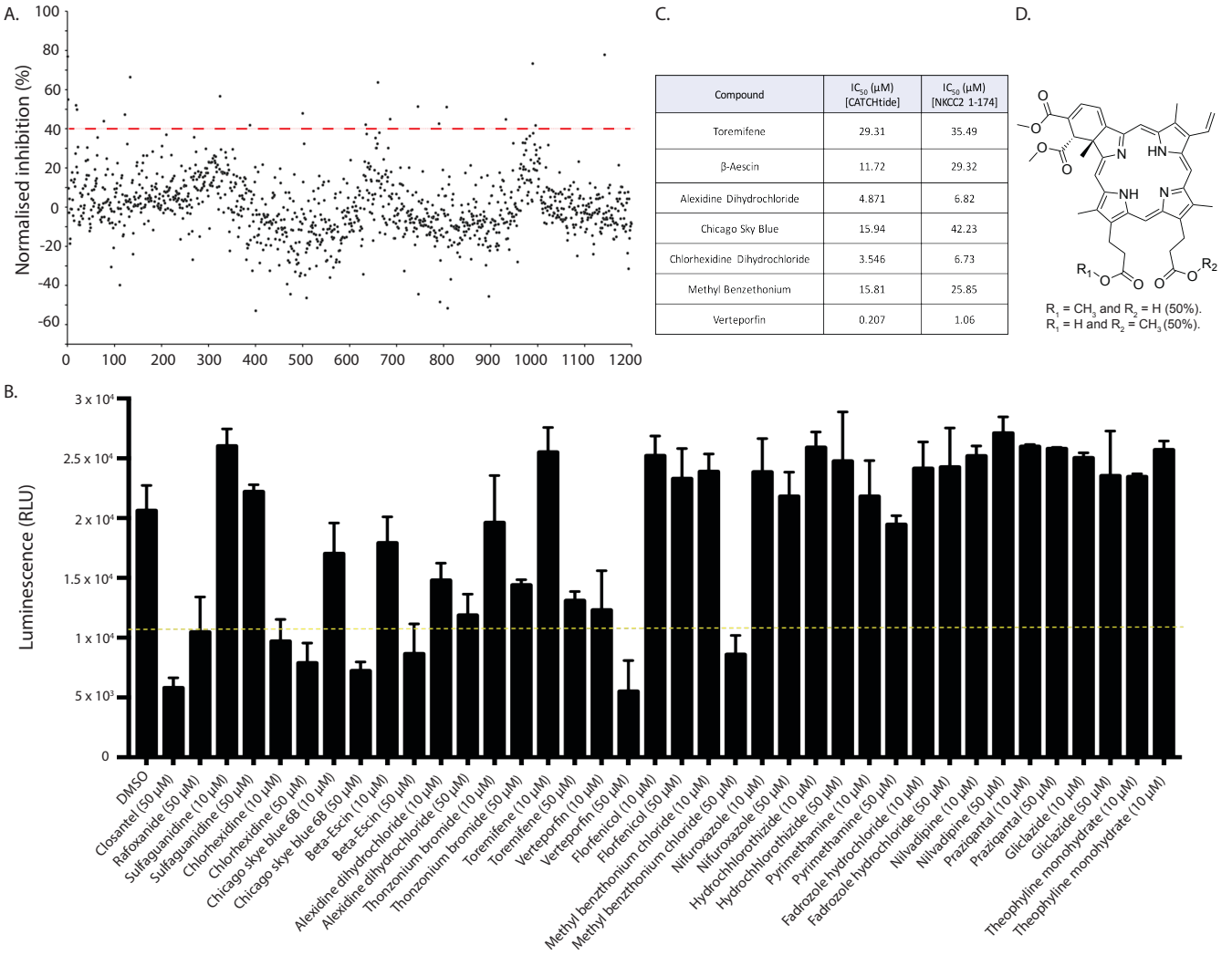

Compound	IC_{50} (µM) [CATCHtide]	IC_{50} (µM) [NKCC2 1-174]
Toremifene	29.31	35.49
β-Aescin	11.72	29.32
Alexidine Dihydrochloride	4.871	6.82
Chicago Sky Blue	15.94	42.23
Chlorhexidine Dihydrochloride	3.546	6.73
Methyl Benzethonium	15.81	25.85
Verteporfin	0.207	1.06

Figure 2. Identification of Verteporfin as an inhibitor of OSR1 T185E in vitro. (**A**) Scatterplots of the primary screening using the developed assay. Dashed line shows the 'hit' selection criteria (≥ 40% Inhibition of OSR1 T185E kinase activity). (**B**) The secondary screening using the developed assay. Compounds were screened at two concentrations 10 and 50 µM in triplicate. Data presented as a mean ± SD. (**C**) *In vitro* IC_{50} values of true hit OSR1 T185E inhibitors using the peptide substrate CATCHtide or the NKCC2 fragment (1-174). (**D**) Chemical structure of Verteporfin, the top hit from the HTS exercise.

emerged as the most potent in vitro inhibitor of OSR1 T185E, IC_{50} = 0.207 µM (**Figure 2C**). Verteporfin exhibited equally potent inhibition of the constitutively active, bacterially expressed human full length SPAK T233E, IC_{50} = 0.330 µM (**Supplementary Figure S5**). Such potency warranted further characterization of Verteporfin as a novel inhibitor of OSR1 and SPAK kinases. Notably, Verteporfin is a mixture of two regioisomers where one of the carboxylic acids is esterified and the other is free as shown in Figure 2D. The compound used in the screening was a 50:50 mixture of the two regioisomers and the subsequent studies in this report employ commercially available Verteporfin, which is a 50:50 mixture of the regioisomers and has an overall 94% purity.

Verteporfin inhibits SPAK and OSR1 in vitro

To understand the mechanism by which Verteporfin inhibits OSR1 T185E, we run the in vitro kinase assay using three different concentrations of ATP (0.01 mM, 0.1 mM and 1 mM). The results showed that Verteporfin inhibition of OSR1 T185E was not significantly influenced by the concentration of ATP indicating that Verteporfin inhibits OSR1 T185E in an ATP-independent manner (**Figure 3A**). Given that Verteporfin has a benzoporphyrin structure with basic nitrogen atoms, we next explored if these would chelate the Mg^{+2} from the kinase assay and this is what led to the observed inhibition. For this, the in vitro kinase assay was run using two different concentrations of $MgCl_2$, 1 mM and 50 mM. The results showed that the inhibition of OSR1 T185E by Verteporfin was not significantly affected by the concentration of $MgCl_2$ suggesting that Verteporfin is not chelating the Mg^{+2} in the kinase assay (**Figures 3B** and **3C**). To further explore this, we next studied the ability of Verteporfin to inhibit the mammalian sterile 20 like kinase 3 (MST3), which belongs to the same family (Ste20) of protein kinases as SPAK and OSR1.[19] The results showed that Verteporfin did not inhibit MST3 even at 100 µM further confirming the inability of Verteporfin to act as a Mg^{+2} chelator in these in vitro kinase assays (**Figure 3D**). Notably, two commercially available analogues of Verteporfin, which contain the porphyrin ring did not inhibit OSR1 T185E in vitro (**Supplementary Figure S6**). Finally, to ensure that Verteporfin was not acting as a protein aggregator, the in vitro kinase assay was run in the absence or presence of 0.05% of the detergent Tween-20. The data showed that there was no dramatic change in the IC_{50} values in both cases indicating that the observed inhibitory effect was not due to the induction of protein (OSR1 T185E) aggregation by Verteporfin (**Figures 3E** and **3F**).

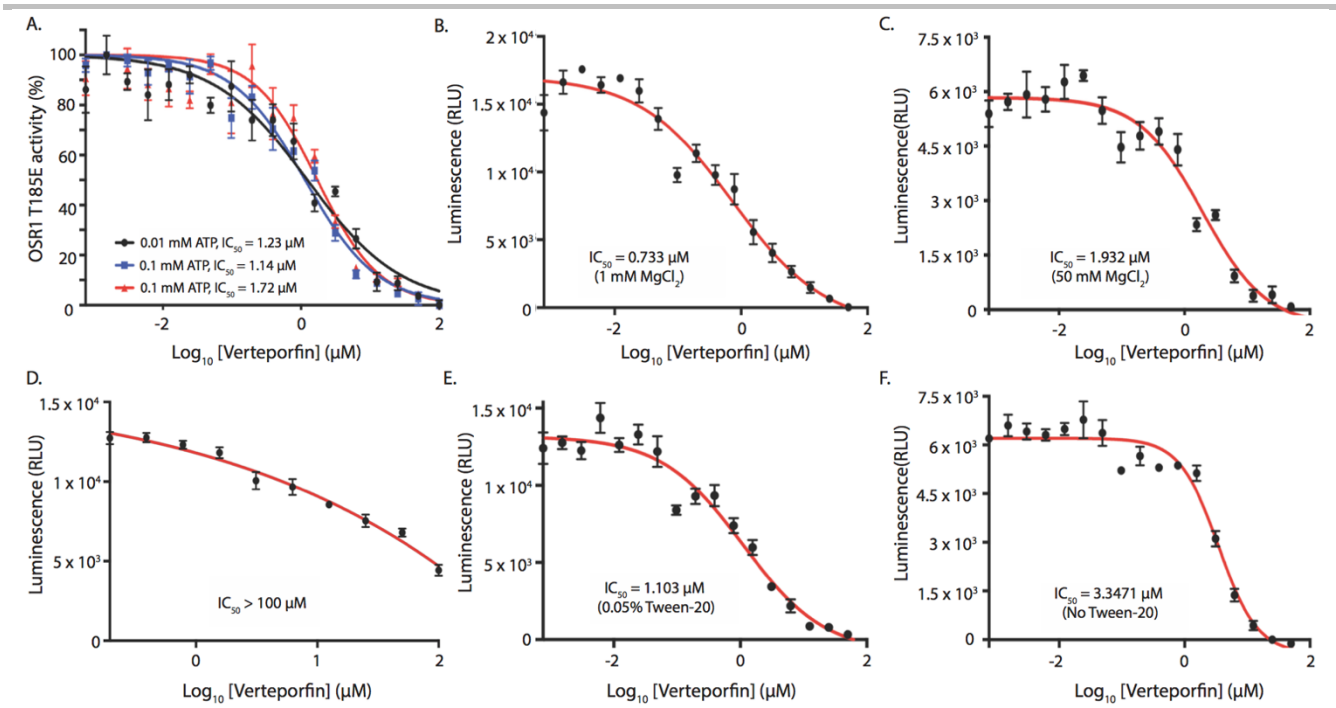

Figure 3. *In vitro* characterization of Verteporfin as an OSR1 kinase inhibitor. (**A**) Verteporfin inhibits OSR1 T185E in vitro in an ATP-independent manner. (**B**) and (**C**) The effect of $MgCl_2$ concentration on the ability of Verteporfin to inhibit OSR1 T185E. (**D**) Verteporfin does not exhibit any *in vitro* inhibition of the constitutively active seine/threonine protein kinase MST3. (**E**) and (**F**) Effect of the detergent Tween-20 on the ability of Verteporfin to inhibit OSR1 T185E. All of the kinase assays were conducted using NKCC2 (1-174) as OSR1 T185E substrate. The data represents a minimum of three independent repeats and every data point is the average of four determinations while the error bars are ± SEM.

As the kinase activity of SPAK and OSR1 is significantly increased by binding to the scaffolding protein MO25,[5] we explored the effect of Verteporfin on the MO25-dependent activation of SPAK T233E and OSR1 T185E in vitro. The results showed that Verteporfin did not affect the ability of MO25 to activate OSR1 T185E in vitro (**Supplementary Figure S7**). Since some reports have implicated that the biological activity of Verteporfin is affected by light,[20] we also studied whether light has an effect on Verteporfin's ability to inhibit OSR1 T185E in vitro. The results showed that carrying the in vitro kinase assay in the dark led to a 3-fold decrease in the ability of Verteporfin to inhibit OSR1 T185E in vitro (**Supplementary Figure S8**).

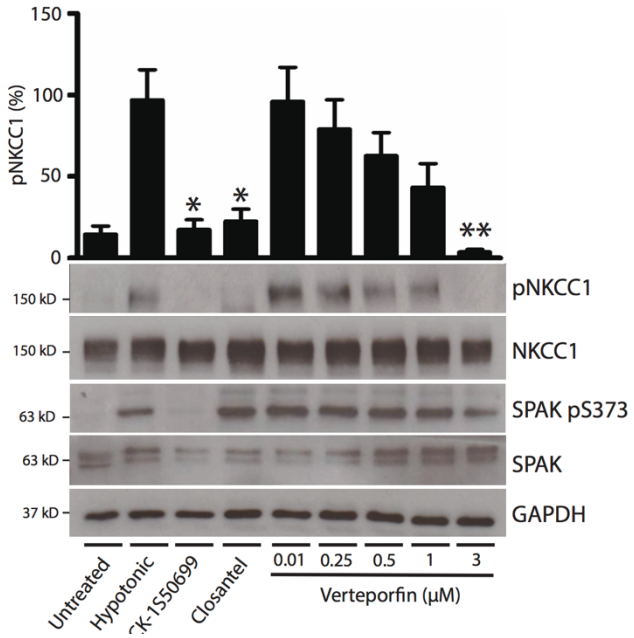

Figure 4. Verteporfin inhibition of SPAK and OSR1 kinases in HEK293 cells. The cells were treated with the vehicle (DMSO) or the indicated inhibitors, STOCK-1S50699 (10 µM), Closantel (20 µM) or Verteporfin at the indicated concentrations. After 30 min incubation, the cells' media was changed to hypotonic buffer for a further 30 min after which the cells were lysed and probed for the indicated proteins. pNKCC1 was quantified relative to GAPDH. The data were reported as mean ± SEM of n = 4; *p < 0.05; ** p < 0.01. A one-way ANOVA test followed by Tukey's test were used to compare the results.

Verteporfin selectivity across 140 protein kinases

To establish the selectivity of Verteporfin towards SPAK and OSR1 kinases, it was run in the MRC PPU Premier Screen of 140 protein kinases (http://www.kinase-screen.mrc.ac.uk/services/premier-screen) at a single concentration of 1 µM. Beyond SPAK and OSR1, the primary HTS screening exercise revealed eight other protein kinases that were potently inhibited with a kinase activity suppression of ≥ 70% at 1 µM. These were the Inhibitor of Nuclear Factor Kappa-B Kinase subunit Epsilon (IKKε), Mammalian STE20-like Protein Kinase 2 (MST2), Germinal Center Kinase (GCK), Mitogen-Activated Protein Kinase Kinase Kinase Kinase 3 (MAP4K3), Mitogen-Activated Protein Kinase 1 (MLK1), Unc-51 Like Autophagy Activating Kinase 1 (ULK1), ULK2 and the Lymphocyte-Specific Protein Tyrosine Kinase (Lck). Further studies into the inhibition of these two important protein kinases are being conducted and will be reported in the future.

Verteporfin inhibits SPAK and OSR1 kinases in cells

Next, the ability of Verteporfin to inhibit SPAK and OSR1 kinases in cells was established (**Figure 4**). HEK293 cells, which express endogenous WNKs, SPAK, OSR1 and MO25 were first treated for 30 minutes with Verteporfin at various concentrations, 10 µM STOCK1S-50699,[12a] a WNK-signaling inhibitor, or 20 µM Closantel, a direct allosteric SPAK/OSR1 kinase inhibitor[12b]. After that, the cells were treated with hypotonic buffer for 30 minutes to activate SPAK and OSR1[3a]. Subsequently, the cells were lysed and probed for SPAK/OSR1-phosphorylation of NKCC1 at residues T203, T207 and T212. As expected, both

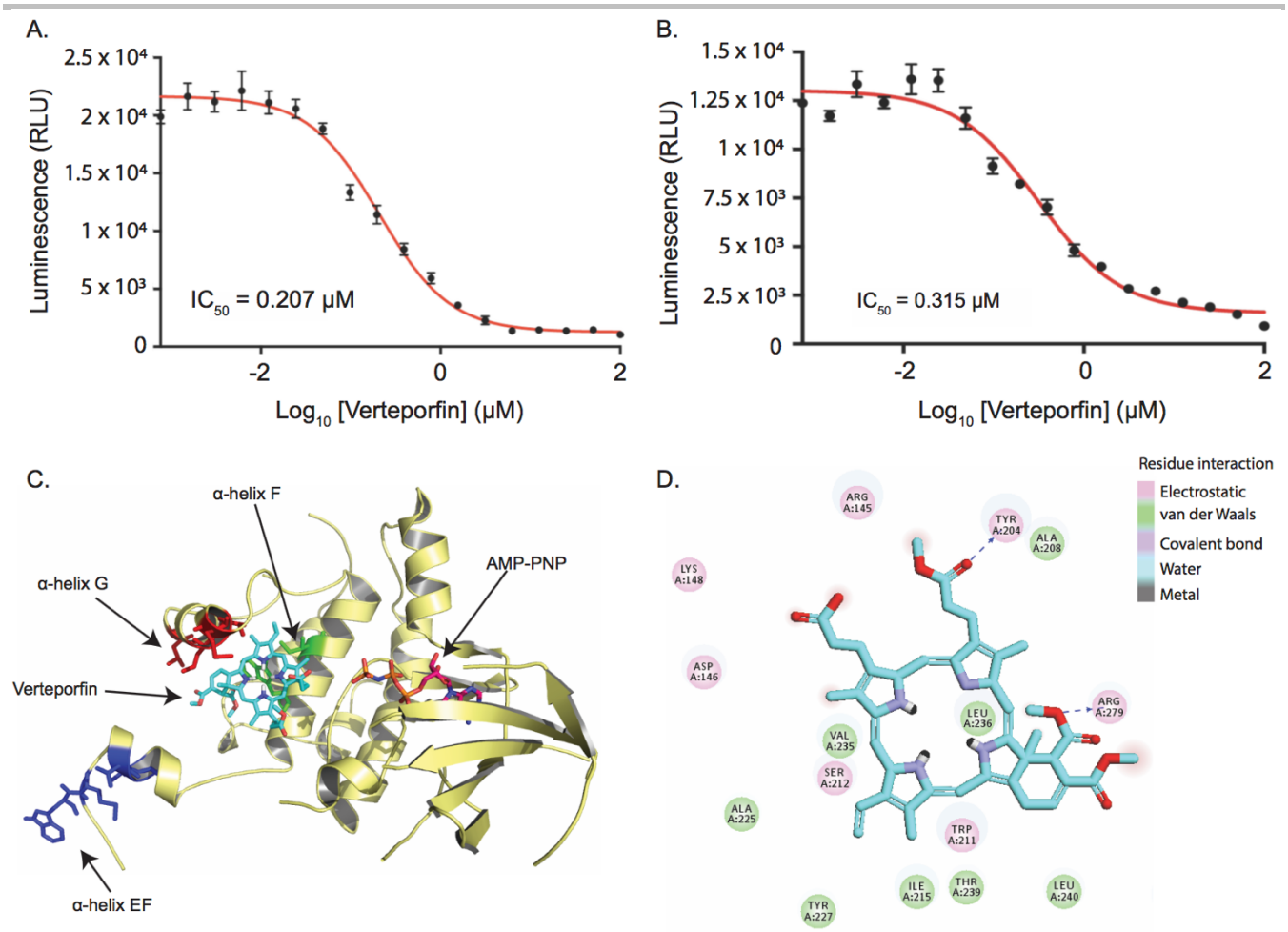

Figure 5. Verteporfin inhibits full length OSR1 T185E by binding to its kinase domain. (**A**) 0.2 µM recombinant full-length human OSR1 T185E 1-527 was purified from *E.coli* was used to phosphorylate the peptide substrate CATCHtide (0.25 mM) in vitro for 30 minutes at 30 °C. 0.1 mM ATP and 10 mM $MgCl_2$ were used in the assay. (B) As in A, but using the CCT truncated recombinant human OSR1 T185E 1-342 instead of the full-length OSR1. Data presented as average of four determinations ± SEM. (C) Docking of Verteporfin (cyan) in the OSR1 kinase domain (PDB ID: 2VWI) shows that it binds to a hydrophobic pocket formed by residues from α-helix G (red) and α-helix F (green). This pocket is called the domain-exchanged kinase dimer, the site for hydrophobic interaction between residues from α-helix EF (blue) of the activation segment of one monomer of OSR1 to another monomer. (D) AutoDock 2D representation of the interaction of Verteporfin with residues at the binding site.

STOCK1S-50699 and Closantel inhibited SPAK and OSR1 kinases as judged by NKCC1 T203, T207 and T212 phosphorylation (**Figure 4**). Impressively, Verteporfin also inhibited NKCC1 phosphorylation at T203, T207 and T212 in a dose-dependent manner though more potently than STOCK1S-50699 and Closantel, as NKCC1 phosphorylation was almost completely abolished at 3 µM of Verteporfin. Critically, Verteporfin inhibition of SPAK and OSR1 kinases did not inhibit SPAK S373 (and OSR1 S325) phosphorylation, which is a specific WNK phosphorylation site. This indicated that Verteporfin is an inhibitor of active SPAK and OSR1 and does not inhibit WNK phosphorylation (and activation) of SPAK and OSR1.

Verteporfin is predicted to bind the activation segment of SPAK and OSR1

As most of the reported SPAK and OSR1 inhibitors are known to bind to the CCT domain of these two kinases,[10] we explored whether Verteporfin also binds the CCT domain. Thus, an in vitro kinase assay comparing Verteporfin inhibitory activity of OSR1 T185E full length and OSR1 T185E 1-342, which lacks the CCT domain, was conducted (**Figure 5A** and **B**). Surprisingly, Verteporfin was able to inhibit both the OSR1 T185E full-length and OSR1 T185E 1-342 with relatively the same potency, IC_{50} = 0.207 µM and 0.305 µM, respectively. This indicated that Verteporfin site of action is not in the CCT domain, but instead in the kinase domain of SPAK and OSR1.

In order to get an idea of the site of Verteporfin binding, we used AutoDock[21] and performed in silico docking of Verteporfin into the crystal structure of OSR1 kinase domain (PDB ID; 2VWI), which is composed of four symmetrical OSR1 molecules arranged as pairs of dimers.[22] At the molecular level, the interaction between the different OSR1 homodimers is mediated by a series of hydrophobic interactions that involve Trp192, Met193, Leu197, and Met198 from helix αEF are occupying a hydrophobic pocket made up from-residues Met233, Val235, Leu236, and Leu240 (helix αG), residues Trp211 and Ile215 (helix αF) of the neighboring molecule (**Figure 5C**). Although the OSR1 kinase domain has been shown to be monomeric in solution, some reports the observation of OSR1 kinase domain forms oligomers in vivo.[23] Despite the fact that OSR1 is activated by WNK phosphorylation, the interactions between OSR1 homodimers is suggested to contribute to the activation of OSR1 akin to that seen with other protein kinases such as the checkpoint kinase 2 (CHK2), lymphocyte-oriented kinase (LOK) and Ste20-like kinase (SLK).[24] Interestingly, the docking results revealed that Verteporfin binds to the flexible domain-exchanged kinase dimer, the site in which the activation segment from each monomer extends to form an extensive intermolecular interface

(**Figure 5C**). As shown in **Figure 5D**, Verteporfin is predicted to form hydrogen bonding with tyrosine 204 (Tyr204) and arginine 279 (Arg279) as well as π-π stacking between tryptophan 211 and the isoindole bicyclic ring of Verteporfin.

Since Verteporfin showed an ability to inhibit eight other protein kinases as discussed above, we also used molecular modelling to explore where Verteporfin binds to these protein kinases. Indeed, we docked Verteporfin into the structures of four protein kinases with crystal structure available in the PDB database (**Supplementary Figure S9**). Akin to what was seen with OSR1, Verteporfin was predicted in silico not to bind these kinases at their ATP sites. In some cases, e.g. MAP4K3, Verteporfin was predicted to bind the dimerization domain of this kinase. Although these in silico predictions seem promising, they need to be further confirmed by crystallography or mutagenesis studies.

Discussion

The compelling in vivo evidence linking the inhibition of SPAK and OSR1 kinases to the regulation of electrolyte balance[7] has made these two protein kinases very attractive molecular targets in the discovery of new antihypertensive drugs.[10] This novel approach for lowering blood pressure became more relevant following the discovery of notable adverse effects associated with the use of WNK kinase inhibitors.[11a] This may be explained by the lack of specificity of these WNK inhibitors across the four humans WNK isoforms[10] and the diverse physiological roles these protein kinases play in humans].[25] The advantage of targeting and inhibiting SPAK and OSR1 kinases instead of WNK kinases is the relative ease of achieving selectivity between these two kinases as they only share 68% sequence similarity.[2]

To discover SPAK and OSR1 kinase inhibitors, we developed a robust OSR1 T185E in vitro kinase assay compatible with HTS technologies and used it to screen a library of 1,200 FDA-approved drugs. This led to the identification of Verteporfin as a potent inhibitor of the constitutively active OSR1 T185E. Notably, this agent also inhibited SPAK T233E in similar potency. Although the activity of Verteporfin has been suggested to be affected by light, the inhibition of OSR1 T185E by Verteporfin was not significantly affected by light as there was only a 3-fold decrease in the inhibitory effect when the kinase activity was carried out in the dark. In terms of the mechanism of inhibition, in silico modelling indicated that Verteporfin inhibits SPAK and OSR1 kinases by binding to their kinase domain instead of their CCT domains. This was an interesting finding as reported SPAK and OSR1 kinase inhibitors bind the CCT domain of these two kinases.[10] In particular, reported SPAK and OSR1 kinase inhibitors, e.g. STOCK50699, bind the primary pocket of these kinases and thus prevent their binding and activation by their upstream kinases, WNKs.[12a] Other SPAK and OSR1 inhibitors such as Rafoxanide are suggested to produce their inhibitory effects by binding the secondary pocket of SPAK and OSR1 kinases.[12c] Unlike these inhibitors, molecular modelling studies suggested that Verteporfin binds an allosteric site adjacent to the kinase domain and the inhibition effect was ATP-independent. This type of allosteric inhibition already exists with other kinase inhibitors. Probably the most similar to this is that of allosteric WNK inhibitors, which also bind to a site adjacent to the ATP binding pocket but are unaffected by ATP binding.[11b] The unique observation made regarding the inhibition of SPAK and OSR1 kinases is that they bind the flexible domain-exchanged kinase dimer. This domain is believed to mediate OSR1 autophosphorylation,[22] and hence may explain how Verteporfin inhibits SPAK and OSR1 kinases. The fact that Verteporfin is likely to bind the flexible domain may also explain our continuous failed efforts of co-crystallizing SPAK and OSR1 kinase domains bound to Verteporfin. As the inhibition of SPAK and OSR1 kinases is known to lower blood pressure,[26] Verteporfin's ability to inhibit these two kinases may explain some recent reports on the low blood pressure observed in animals that underwent treatment with Verteporfin.[27]

The screening of Verteporfin against a panel of 140 protein kinases indicated that it also potently inhibited a range of protein kinases that are implicated in many important physiological processes. Some of the proteins these proteins have been implicated in inflammation, immune responses and cancer, e.g. IKKε,[28] MST2,[29] ULK1,[30] and MAP4K3[31]. Notably, the inhibition of the protein kinase MST2, a component of the Hippo signalling pathway,[32] may contribute to the previously reported anticancer activities[33] of Verteporfin that have been attributed to targeting this signalling cascade, specifically the inhibition of TEAD (Transcriptional Enhancer Associate Domain) interaction with YAP (Yes-Associated Protein).[34] Nevertheless, Verteporfin's ability to inhibit a selection of protein kinases may lead to undesired side effects and could complicate the ongoing in vivo studies examining the pharmacological properties of this clinical agent.[35]

Conclusion

In this work, we showed that the clinically used agent Verteporfin is a potent inhibitor of SPAK and OSR1 kinases in vitro and in cells. It inhibits these kinases in an ATP-independent manner through the binding to a site remote from their CCT domains. In silico modelling indicated that Verteporfin binds the flexible dimerization domain of SPAK and OSR1. Although in a kinase screen panel, Verteporfin also inhibited eight other protein kinases, it still has the potential to be a powerful tool in studying SPAK and OSR1 signaling as to date it is the most potent reported inhibitor of these two important protein kinases.

Experimental Section

Reagents. Verteporfin (94% purity), its analogues [protoporphyrin IX dimethyl ester (90% purity) and 2,3,7,8,12,13,17,18-Octaethyl-21*H*,23*H*-porphine (97% purity)], Closantel, Rafoxanide, tissue culture and protein expression reagents were purchased from Sigma–Aldrich. GST PreScission protease enzyme and glutathione-sepharose beads were purchased from GE Healthcare. CATCHtide were purchased from GLS Peptide Synthesis (China). The ADP-Glo™ Assay was purchased from Promega (UK). STOCK1S-50699 and DNA clones were purchased from the MRC PPU Services and Reagents (Dundee, UK).

Buffers. Cell lysis buffer: 50 mM Tris:HCl (pH 7.5), 1 mM EDTA, 1 mM EGTA, 50 mM sodium fluoride, 5 mM sodium pyrophosphate, 1 mM sodium orthovanadate, 1% (w/v) Nonidet P40, 0.27mM sucrose supplemented with fresh 0.1% (v/v) 2-mercaptoethanol, 0.1 mM PMSF, 1 mM benzamidine. Bacterial lysis buffer: 50 mM Tris:HCl (pH 7.5), 150 mM NaCl, 1 mM EGTA, 1 mM EDTA, 0.27 M sucrose supplemented with fresh 0.1 mM PMSF, 1 mM benzamidine, 0.5 mg/mL lysosome, 0.3 mg/mL 1 DNase and 0.01% (v/v) 2-mercaptoethanol. Buffer A: 50 mM Tris:HCl (pH 7.5), 0.1 mM EGTA supplemented with fresh 0.1% (v/v) 2-mercaptoethanol. Normal buffer: Consists of bacterial lysis buffer without lysozyme and DNase. High-salt buffer: normal buffer with 500 mM NaCl. Protein elution buffer: buffer A (pH 8), 150 mM NaCl and 20 mM reduced

glutathione or preScission protease enzyme. TBS-T buffer: 50 mM Tris:base (pH 7.5), 150 mM NaCl and 0.2% (v/v) Tween-20. Running buffer: 34.6 mM SDS, 25 mM Tris·Base and 1.92M glycine. Transfer buffer: 48 mM Tris·Base, 39 mM glycine containing 20% (v/v) methanol. Hypotonic low chloride buffer: Consists of 67.5 mM sodium gluconate, 2.5 mM potassium gluconate, 0.25 mM $CaCl_2$, 0.25 mM $MgCl_2$, 0.5 mM Na_2HPO_4, 0.5 mM Na_2SO_4 and 7.5 mM HEPES. SDS sample buffer (4X): Consists of 40% glycerol, 240 mM Tris:HCl (pH 6.8), 8% SDS, 0.04% bromophenol blue and 5% 2-mercaptoethanol.

Antibodies. Anti-SPAK pS373 [S670B], anti-total-SPAK [S551D], anti-NKCC1 pT203+pT207+pT212) [S763B] and anti-total NKCC1 [DU 6146] were purchased from the MRC PPU Services and Reagents (Dundee, UK). Anti-GAPDH [2118] was purchased from Cell Signalling Technology. Anti-rabbit [31460] and anti-sheep [31480] secondary antibodies conjugated to HRP were purchased from Thermo Scientific.

DNA plasmids. pGEX-OSR1 T185E full-length [DU6231], pGEX-OSR1 T185E (1-342) [DU6363], pGEX-SPAK T233E full-length [DU6246] and pGEX-NKCC2 (1-174) [DU13763] were all purchased from the MRC PPU Services and Reagents (Dundee, UK).

Protein expression and purification. pGEX-6P-1 constructs encoding N-terminal GST-tagged proteins were transformed into BL21 (DE3) E.coli. One litre of transformed BL21 E. coli cells was grown at 37 °C at 180 rpm in Luria Broth media containing 100 µg/mL ampicillin until reaching an OD_{600} of 0.7. Protein expression was induced by addition of 250 µM IPTG. Then, cells were cultured for an additional 16 hours at 26 °C at 180 rpm before collecting them by centrifugation at 3,500g at 4 °C for 30 minutes. The cell pellet was resuspended in 50 mL ice-cold bacterial lysis buffer and incubated in ice path at 4°C for 30 minutes. Bacteria were lysed by sonication, for 30 seconds on/off round six times. Lysates were centrifuged at 25000*g* at 4 °C for 30 minutes. The supernatant was collected and incubated overnight with 2 mL/L of glutathione-Sepharose beads (pre-washed with lysis buffer) to affinity purified GST-tagged proteins. The beads were then washed twice with normal buffer, high salt buffer and buffer A, respectively. GST proteins were eluted with elution buffer containing 20mM reduced L-glutathione. NKCC2 1-174 was eluted with elution buffer containing preScission protease enzyme. Proteins were concentrated to 100-500 µL with amicon ultra-15 centrifugal filter units (3 kDa and 10 kDa cut-off). Proteins concentrations were measured by Bradford assay. Proteins yield and purity were confirmed by SDS-PAGE and Coomassie staining using different concentrations of bovine serum albumin (BSA) as standards.[5]

Cell culture and treatment with inhibitors. Human embryonic kidney 293 cells were cultured on 6-well plates in Dulbecco's modified Eagle's medium (DMEM) supplemented with 10% (v/v) fetal bovine serum, 2 mM L-glutamine, 100 units/mL penicillin and 0.1 mg/mL streptomycin at 37 °C in a humidified 5% CO_2 incubator. For the inhibition assay, 75% confluent cells were incubated with DMSO as a vehicle control or compounds at indicated concentrations for 30 minutes using Closantel and STOCK1S-50699 as positive controls. Then WNK signalling was stimulated with low-chloride hypotonic buffer for 30 minutes. Then cells were washed with 1 mL phosphate-buffered saline (PBS) and lysed subsequently with 150 µL ice-cold cells lysis buffer per well and centrifuged at 12,000*g* at 4 °C for 10 minutes to collect the proteins. The proteins concentrations were measured using standard Bradford assay. Then, protein samples were denatured for 5 minutes at 90 °C with 1X SDS buffer and subjected to SDS-PAGE. Final DMSO concentration was 0.1%.

Immunoblotting. SDS Samples were subjected to 10% SDS-PAGE. Then proteins transferred from gel on to nitrocellulose membranes. The membranes were then blocked with blocking buffer for 45 minutes on platform shaker. Then, the membranes were incubated with primary antibody (anti-phospho-SPAK (2 µg/mL), anti-total-SPAK (2 µg/mL), anti-phospho-NKCC1 (2 µg/mL) and anti-total NKCC1 (2 µg/mL) in 5% (w/v) dried skimmed milk in TBS-T, anti-GAPDH (1:1000) and anti-GST (1:500) in 10% (w/v) bovine serum albumin (BSA) /TBS-T) for 1 hour at room temperature or overnight at 4 °C. Then membranes were washed four times with TBS-T and incubated with secondary antibody (anti-sheep (1:2000) in 5% (w/v) dried skimmed milk in TBS-T and anti-rabbit (1:2500) in 10% (w/v) BSA/TBS-T). The membranes then washed four times with TBS-T. The detection was done by adding enhanced chemiluminescence reagent to the membranes and developing an auto-radiographic film. The bands intensities were and quantified by ImageJ software (NIH) and analysis with GraphPadPrism 6.0.

Docking studies. Autodock [31] Vina 1.1.2 was used to dock Verteporfin into OSR1 kinase domain (PDB ID: 2VWI). Verteporfin SDF file was download from PubChem (PubChem CID: 5362420). The protein and compound PDB files were initially prepared and visualized with Discovery Studio 4.5 (Accelrys, San Diego, CA, USA) and then converted into PDBQT format using AutoDock Tool 1.5.6.[36] Unbiased docking approach in which the grid box was centralized to cover the whole protein, was performed using default settings as described by developers. The docking results were visualized and analyzed using Discovery Studio 4.5 and PyMOL Molecular Graphics System 1.3.

ADP-Glo™ (HTS) kinase assay. The assay was performed in 384-well plate format by incubating 1 µl of either DMSO or different concentrations of the inhibitors with 0.2 µM purified proteins in a 5 µL total reaction volume containing 50 mM Tris-HCl, 10 mM $MgCl_2$, 0.1% (v/v) 2-mercaptoethanol, 0.05% Tween-20, and 0.1 mM ATP in buffer A employing GST cleaved NKCC2 1-174 or CATCHtide (RRHYYYDTHTNTYYLR-TFGHNTRR) as substrates at 5 µM and 250 µM final concentrations, respectively. The kinase reaction was carried out in a white round-bottom 384-well plate (Greiner) at 30 °C for 30 minutes with gentle agitation on microplate shaker incubator. The kinase activity was assayed using ADP-Glo™ kinase assay according to the manufacturer's protocol.[14] The plate was subsequently read on a BMG FLUOstar Omega plate reader. In the case of running the kinase assay in the dark, the kinase assay plate was covered with aluminium foil prior to adding Verteporfin and then kept covered during the running of the assay and until the reading of the assay results in the BMG FLUOstar Omega plate reader. For chemical library screening, assay was performed in duplicate following the HTS screening data illustrated below. For inhibition studies, increasing concentrations of each compound were tested in four replicates with at least ten to eighteen data points per curve. For studying the effect of Verteporfin on MST3 kinase, the kinase assay was conducted with the same protocol using 0.1 µM of recombinant MST3 (1 - 431) [MRC PPU Services and Reagents (Dundee, UK)] with 0.3 mg/mL Myelin basic protein (MBP) (Sigma Aldrich) as a substrate as reported.[5] Curve fitting and data analysis was completed with GraphPadPrism 6.0. Final DMSO concentration was 4%.

HTS assay performance. The assay parameters were calculated according to the following equations[17]:

$$Z' = 1 - \frac{3\,\sigma\ \text{positive} + 3\,\sigma\ \text{negative}}{|\,\mu\ \text{positive} - \mu\ \text{negative}|}$$

$$S/N = 1 - \frac{\mu\ \text{negative} - \mu\ \text{positive}}{\sigma\ \text{positive}}$$

$$S/B = 1 - \frac{\mu\ \text{negative}}{\mu\ \text{positive}}$$

Where σ and µ are the standard deviations and means of the positive (total reaction mixture with NKCC2 1-174 substrate in absence of OSR1 T185E kinase) and negative (total reaction mixture with NKCC2 (1-174) substrate in presence of OSR1 T185E kinase) controls, respectively. The reported values were the average of three independent experiments of sixteen replicates performed on different days.

Post screening, in addition to the Z' factor, the signal window (SW) and coefficient of variation (CV%) were determined for each plate based on the following equations:

$$SW = 1 - \frac{\mu\ \text{negative} - \mu\ \text{positive}}{\sigma\ \text{positive}}$$

$$CV\% = \left(\frac{\sigma\ \text{negative}}{\mu\ \text{negative}}\right)$$

The reported values for each plate were the average for two plates with sixteen replicates per each.

Acknowledgements

We are also grateful to the Protein Expression Facility (University of Birmingham) for help with protein production. M.A.A. is funded

by a PhD studentship from the Ministry of Education in Saudi Arabia and Prince Sattam Bin Abdulaziz University.

Keywords: SPAK • OSR1 • WNK • High throughput • Inhibitor

References

[1] a) D. R. Alessi, J. Zhang, A. Khanna, T. Hochdorfer, Y. Shang, K. T. Kahle, *Sci. Signal.* **2014**, *7*, re3; b) J. Hadchouel, D. H. Ellison, G. Gamba, *Ann. Rev. Physiol.* **2016**, *78*, 367-389; c) C. Richardson, D. R. Alessi, *J. Cell Sci.* **2008**, *121*, 3293-3304.

[2] A. C. Vitari, J. Thastrup, F. H. Rafiqi, M. Deak, N. A. Morrice, H. K. Karlsson, D. R. Alessi, *Biochem. J.* **2006**, *397*, 223-231.

[3] a) A. Zagorska, E. Pozo-Guisado, J. Boudeau, A. C. Vitari, F. H. Rafiqi, J. Thastrup, M. Deak, D. G. Campbell, N. A. Morrice, A. R. Prescott, D. R. Alessi, *J. Cell Biol.* **2007**, *176*, 89-100; b) T. Moriguchi, S. Urushiyama, N. Hisamoto, S. Iemura, S. Uchida, T. Natsume, K. Matsumoto, H. Shibuya, *J. Biol. Chem.* **2005**, *280*, 42685-42693.

[4] a) H. Miyamoto, A. Matsushiro, M. Nozaki, *Mol. Reprod. Dev.* **1993**, *34*, 1-7; b) M. Nozaki, Y. Onishi, S. Togashi, H. Miyamoto, *DNA Cell Biol.* **1996**, *15*, 505-509.

[5] B. M. Filippi, P. de los Heros, Y. Mehellou, I. Navratilova, R. Gourlay, M. Deak, L. Plater, R. Toth, E. Zeqiraj, D. R. Alessi, *EMBO J.* **2011**, *30*, 1730-1741.

[6] F. H. Wilson, S. Disse-Nicodeme, K. A. Choate, K. Ishikawa, C. Nelson-Williams, I. Desitter, M. Gunel, D. V. Milford, G. W. Lipkin, J. M. Achard, M. P. Feely, B. Dussol, Y. Berland, R. J. Unwin, H. Mayan, D. B. Simon, Z. Farfel, X. Jeunemaitre, R. P. Lifton, *Science* **2001**, *293*, 1107-1112.

[7] M. Murthy, T. Kurz, K. M. O'Shaughnessy, *Cell. Mol. Life Sci.* **2017**, *74*, 1261-1280.

[8] a) A. Ohta, F. R. Schumacher, Y. Mehellou, C. Johnson, A. Knebel, T. J. Macartney, N. T. Wood, D. R. Alessi, T. Kurz, *Biochem. J.* **2013**, *451*, 111-122; b) M. Wakabayashi, T. Mori, K. Isobe, E. Sohara, K. Susa, Y. Araki, M. Chiga, E. Kikuchi, N. Nomura, Y. Mori, H. Matsuo, T. Murata, S. Nomura, T. Asano, H. Kawaguchi, S. Nonoyama, T. Rai, S. Sasaki, S. Uchida, *Cell Rep.* **2013**, *3*, 858-868; c) S. Shibata, J. Zhang, J. Puthumana, K. L. Stone, R. P. Lifton, *Proc. Nat. Acad. Sci. USA* **2013**, *110*, 7838-7843.

[9] a) L. M. Boyden, M. Choi, K. A. Choate, C. J. Nelson-Williams, A. Farhi, H. R. Toka, I. R. Tikhonova, R. Bjornson, S. M. Mane, G. Colussi, M. Lebel, R. D. Gordon, B. A. Semmekrot, A. Poujol, M. J. Valimaki, M. E. De Ferrari, S. A. Sanjad, M. Gutkin, F. E. Karet, J. R. Tucci, J. R. Stockigt, K. M. Keppler-Noreuil, C. C. Porter, S. K. Anand, M. L. Whiteford, I. D. Davis, S. B. Dewar, A. Bettinelli, J. J. Fadrowski, C. W. Belsha, T. E. Hunley, R. D. Nelson, H. Trachtman, T. R. Cole, M. Pinsk, D. Bockenhauer, M. Shenoy, P. Vaidyanathan, J. W. Foreman, M. Rasoulpour, F. Thameem, H. Z. Al-Shahrouri, J. Radhakrishnan, A. G. Gharavi, B. Goilav, R. P. Lifton, *Nature* **2012**, *482*, 98-102; b) H. Louis-Dit-Picard, J. Barc, D. Trujillano, S. Miserey-Lenkei, N. Bouatia-Naji, O. Pylypenko, G. Beaurain, A. Bonnefond, O. Sand, C. Simian, E. Vidal-Petiot, C. Soukaseum, C. Mandet, F. Broux, O. Chabre, M. Delahousse, V. Esnault, B. Fiquet, P. Houillier, C. I. Bagnis, J. Koenig, M. Konrad, P. Landais, C. Mourani, P. Niaudet, V. Probst, C. Thauvin, R. J. Unwin, S. D. Soroka, G. Ehret, S. Ossowski, M. Caulfield, P. Bruneval, X. Estivill, P. Froguel, J. Hadchouel, J. J. Schott, X. Jeunemaitre, *Nature Genet.* **2012**, *44*, 456-460.

[10] M. A. AlAmri, H. Kadri, B. A. Dhiani, S. Mahmood, A. Elzwawi, Y. Mehellou, *ChemMedChem* **2017**, *12*, 1677-1686.

[11] a) K. Yamada, H. M. Park, D. F. Rigel, K. DiPetrillo, E. J. Whalen, A. Anisowicz, M. Beil, J. Berstler, C. E. Brocklehurst, D. A. Burdick, S. L. Caplan, M. P. Capparelli, G. Chen, W. Chen, B. Dale, L. Deng, F. Fu, N. Hamamatsu, K. Harasaki, T. Herr, P. Hoffmann, Q. Y. Hu, W. J. Huang, N. Idamakanti, H. Imase, Y. Iwaki, M. Jain, J. Jeyaseelan, M. Kato, V. K. Kaushik, D. Kohls, V. Kunjathoor, D. LaSala, J. Lee, J. Liu, Y. Luo, F. Ma, R. Mo, S. Mowbray, M. Mogi, F. Ossola, P. Pandey, S. J. Patel, S. Raghavan, B. Salem, Y. H. Shanado, G. M. Trakshel, G. Turner, H. Wakai, C. Wang, S. Weldon, J. B. Wielicki, X. Xie, L. Xu, Y. I. Yagi, K. Yasoshima, J. Yin, D. Yowe, J. H. Zhang, G. Zheng, L. Monovich, *Nature Chem. Biol.* **2016**, *12*, 896-898; b) K. Yamada, J. H. Zhang, X. Xie, J. Reinhardt, A. Q. Xie, D. LaSala, D. Kohls, D. Yowe, D. Burdick, H. Yoshisue, H. Wakai, I. Schmidt, J. Gunawan, K. Yasoshima, Q. K. Yue, M. Kato, M. Mogi, N. Idamakanti, N. Kreder, P. Drueckes, P. Pandey, T. Kawanami, W. Huang, Y. I. Yagi, Z. Deng, H. M. Park, *ACS Chem. Biol.* **2016**, *11*, 3338-3346.

[12] a) T. Mori, E. Kikuchi, Y. Watanabe, S. Fujii, M. Ishigami-Yuasa, H. Kagechika, E. Sohara, T. Rai, S. Sasaki, S. Uchida, *Biochem. J.* **2013**, *455*, 339-345; b) E. Kikuchi, T. Mori, M. Zeniya, K. Isobe, M. Ishigami-Yuasa, S. Fujii, H. Kagechika, T. Ishihara, T. Mizushima, S. Sasaki, E. Sohara, T. Rai, S. Uchida, *J. Am. Soc. Nephrol.* **2015**, *26*, 1525-1536; c) M. A. AlAmri, H. Kadri, L. J. Alderwick, N. S. Simpkins, Y. Mehellou, *ChemMedChem* **2017**, *12*, 639-645.

[13] P. de Los Heros, D. R. Alessi, R. Gourlay, D. G. Campbell, M. Deak, T. J. Macartney, K. T. Kahle, J. Zhang, *Biochem. J.* **2014**, *458*, 559-573.

[14] H. Zegzouti, M. Zdanovskaia, K. Hsiao, S. A. Goueli, *Assay Drug Dev. Techn.* **2009**, *7*, 560-572.

[15] A. C. Vitari, M. Deak, N. A. Morrice, D. R. Alessi, *Biochem. J.* **2005**, *391*, 17-24.

[16] C. Richardson, K. Sakamoto, P. de los Heros, M. Deak, D. G. Campbell, A. R. Prescott, D. R. Alessi, *J. Cell Sci.* **2011**, *124*, 789-800.

[17] J. H. Zhang, T. D. Chung, K. R. Oldenburg, *J. Biomol. Scr.* **1999**, *4*, 67-73.

[18] a) M. A. Awan, S. A. Tarin, *Surgeon* **2006**, *4*, 231-236; b) C. Fenton, C. M. Perry, *Drugs Aging* **2006**, *23*, 421-445.

[19] L. R. Pearce, D. Komander, D. R. Alessi, *Nature Rev. Mol. Cell Biol.* **2010**, *11*, 9-22.

[20] a) E. Donohue, A. D. Balgi, M. Komatsu, M. Roberge, *PLoS One* **2014**, *9*, e114964; b) E. K. Konstantinou, S. Notomi, C. Kosmidou, K. Brodowska, A. Al-Moujahed, F. Nicolaou, P. Tsoka, E. Gragoudas, J. W. Miller, L. H. Young, D. G. Vavvas, *Sci. Rep.* **2017**, *7*, 46581.

[21] D. S. Goodsell, G. M. Morris, A. J. Olson, *J. Mol. Recognit.* **1996**, *9*, 1-5.

[22] F. Villa, M. Deak, D. R. Alessi, D. M. van Aalten, *Proteins* **2008**, *73*, 1082-1087.

[23] A. N. Anselmo, S. Earnest, W. Chen, Y. C. Juang, S. C. Kim, Y. Zhao, M. H. Cobb, *Proc. Nat. Acad. Sci. USA* **2006**, *103*, 10883-10888.

[24] a) A. W. Oliver, A. Paul, K. J. Boxall, S. E. Barrie, G. W. Aherne, M. D. Garrett, S. Mittnacht, L. H. Pearl, *EMBO J.* **2006**, *25*, 3179-3190; b) A. C. Pike, P. Rellos, F. H. Niesen, A. Turnbull, A. W. Oliver, S. A. Parker, B. E. Turk, L. H. Pearl, S. Knapp, *EMBO J.* **2008**, *27*, 704-714.

[25] a) A. R. Rodan, A. Jenny, *Curr. Top. Dev. Biol.* **2017**, *123*, 1-47; b) M. Shekarabi, J. Zhang, A. R. Khanna, D. H. Ellison, E. Delpire, K. T. Kahle, *Cell Metab.* **2017**, *25*, 285-299; c) C. S. Wilson, A. A. Mongin, *Neurosc. Lett.* **2018**, DOI: 10.1016/j.neulet.2018.01.012.

[26] F. H. Rafiqi, A. M. Zuber, M. Glover, C. Richardson, S. Fleming, S. Jovanovic, A. Jovanovic, K. M. O'Shaughnessy, D. R. Alessi, *EMBO Mol. Med.* **2010**, *2*, 63-75.

[27] S. K. Charisis, I. Naoumidi, H. S. Ginis, M. K. Tsilimbaris, *Invest. Ophthalmol. Vis. Sci.* **2007**, *47*, 3970.

[28] K. Verhelst, L. Verstrepen, I. Carpentier, R. Beyaert, *Biochem. Pharmacol.* **2013**, *85*, 873-880.

[29] E. O'Neill, W. Kolch, *Cell Cycle* **2005**, *4*, 365-367.

[30] D. Saleiro, E. M. Kosciuczuk, L. C. Platanias, *Cytokine Growth Factor Rev.* **2016**, *29*, 17-22.

[31] H. C. Chuang, X. Wang, T. H. Tan, *Adv. Immunol.* **2016**, *129*, 277-314.

[32] D. Pan, *Dev. Cell* **2010**, *19*, 491-505.

[33] F. Gibault, M. Corvaisier, F. Bailly, G. Huet, P. Melnyk, P. Cotelle, *Curr. Med. Chem.* **2016**, *23*, 1171-1184.

[34] Y. Liu-Chittenden, B. Huang, J. S. Shim, Q. Chen, S. J. Lee, R. A. Anders, J. O. Liu, D. Pan, *Genes Dev.* **2012**, *26*, 1300-1305.

[35] a) M. T. Huggett, M. Jermyn, A. Gillams, R. Illing, S. Mosse, M. Novelli, E. Kent, S. G. Bown, T. Hasan, B. W. Pogue, S. P. Pereira, *Br. J. Cancer* **2014**, *110*, 1698-1704; b) J. Feng, J. Gou, J. Jia, T. Yi, T. Cui, Z. Li, *OncoTargets Ther.* **2016**, *9*, 5371-5381.

[36] M. F. Sanner, *J. Mol. Graph. Model.* **1999**, *17*, 57-61.

Table of Contents

SPAK and OSR1 are two serine/threonine protein kinases that control the function of a series of ion co-transporters and hence cellular electrolyte balance. Animal models with impaired SPAK and OSR1 signalling have been shown to exhibit reduced blood pressure. In this work, we report the identification and characterisation of the clinically used agent Verteporfin as a potent inhibitor of SPAK and OSR1 kinases.

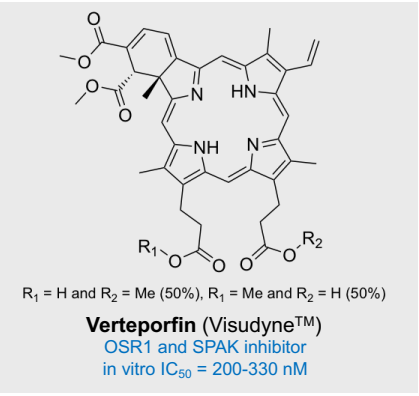

R_1 = H and R_2 = Me (50%), R_1 = Me and R_2 = H (50%)

Verteporfin (Visudyne™)
OSR1 and SPAK inhibitor
in vitro IC_{50} = 200-330 nM

*Mubarak A. AlAmri, Hachemi Kadri, Luke J. Alderwick, Mark Jeeves, Youcef Mehellou,**

Page No. – Page No.

The Photosensitizing Clinical Agent Verteporfin is an Inhibitor of SPAK and OSR1 Kinases

Supporting Information

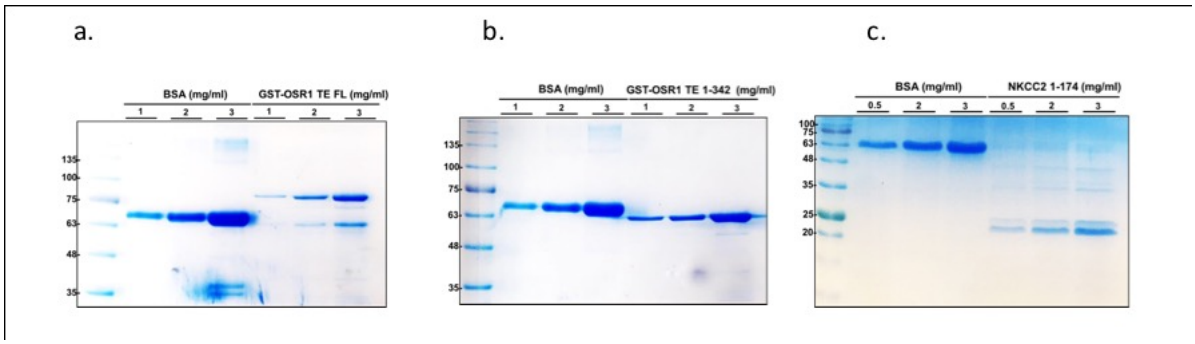

Figure S1. SDS-PAGE gels of the proteins used in this study. (**A**) GST-OSR1 T185E FL (**B**) GST-OSR1 T185E 1-342 (**C**) NKCC2 1-174 purifications using Coomassie blue stain. BSA (Sigma Aldrich, cat#A2153, purity ≥ 96% (agarose gel electrophoresis) was used at different concentrations as standards for proteins yield and purity determination.

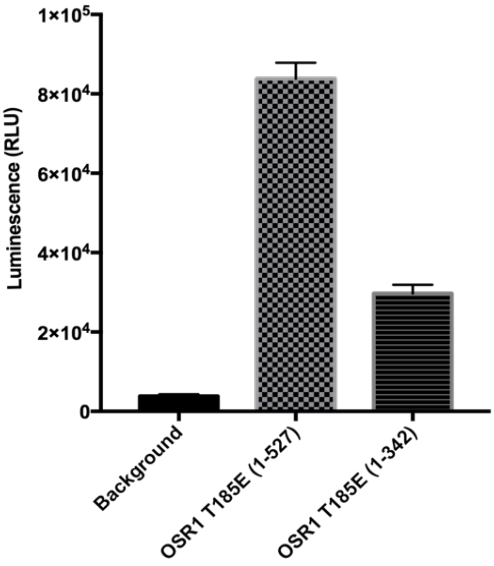

Figure S2. Optimization of the in vitro OSR1 T185E HTS ADP-GLO™ kinase assay using CATCHtide as a substrate. The in vitro kinase assay was performed in 384-well plate in a total volume of 5 µl comprising 0.2 µM OSR1 T185E full length or truncated OSR1 T185E 1-342, 250 µM CATCHtide. 50 mM Tris-HCl, 10 mM $MgCl_2$, 0.1% (v/v) 2-mercaptoethanol, 0.05% Tween-20, and 0.1 mM ATP in buffer A.

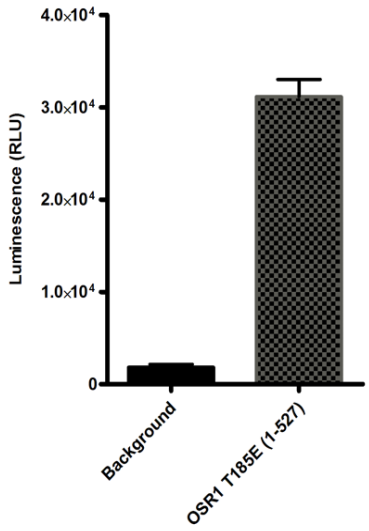

Figure S3. Optimization of the in vitro OSR1 T185E HTS ADP-GLO™ kinase assay using human NKCC2 (1-174) as a substrate. The in vitro kinase assay was performed in 384-well plate in a total volume of 5 µl comprising 0.2 µM OSR1 T185E full length or truncated OSR1 T185E 1-342, 5 µM recombinant human NKCC2 (1-174). 50 mM Tris-HCl, 10 mM $MgCl_2$, 0.1% (v/v) 2-mercaptoethanol, 0.05% Tween-20, and 0.1 mM ATP in buffer A.

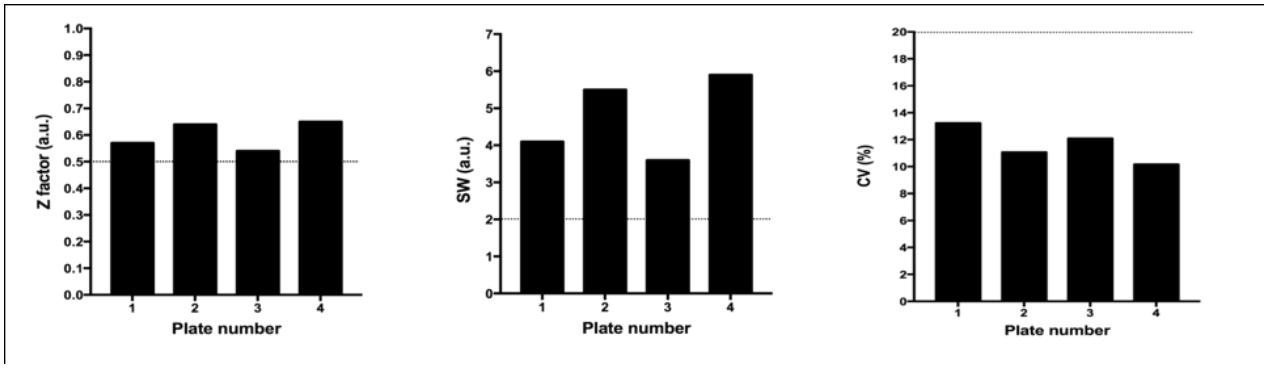

Figure S4. Post-screening assay parameters. Post screening assay parameters. **(Left)**The z' factor, **(Middle)** signal window (SW), and **(Right)** coefficient of variation (CV) of each plate were calculated and then compared with the minimum pass criteria. Dashed lines show the minimum pass criteria (z' > 0.5, SW > 2, CV < 20%).

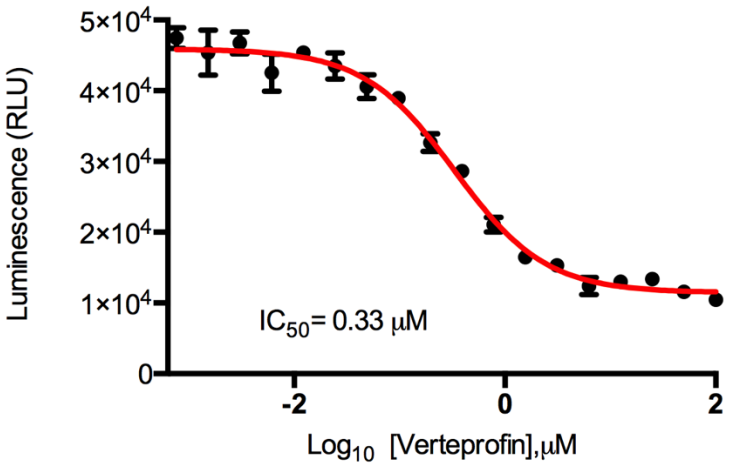

Figure S5. In vitro inhibition of SPAK T233E by Verteporfin. 0.2 µM recombinant full-length human SPAK T185E 1-547 was purified from *E.coli* was used to phosphorylate the peptide substrate CATCHtide (250 µM) in vitro for 30 minutes at 30 °C. 0.1 mM ATP and 10 mM $MgCl_2$ were used in the assay as described under the Reagents and Methods section.

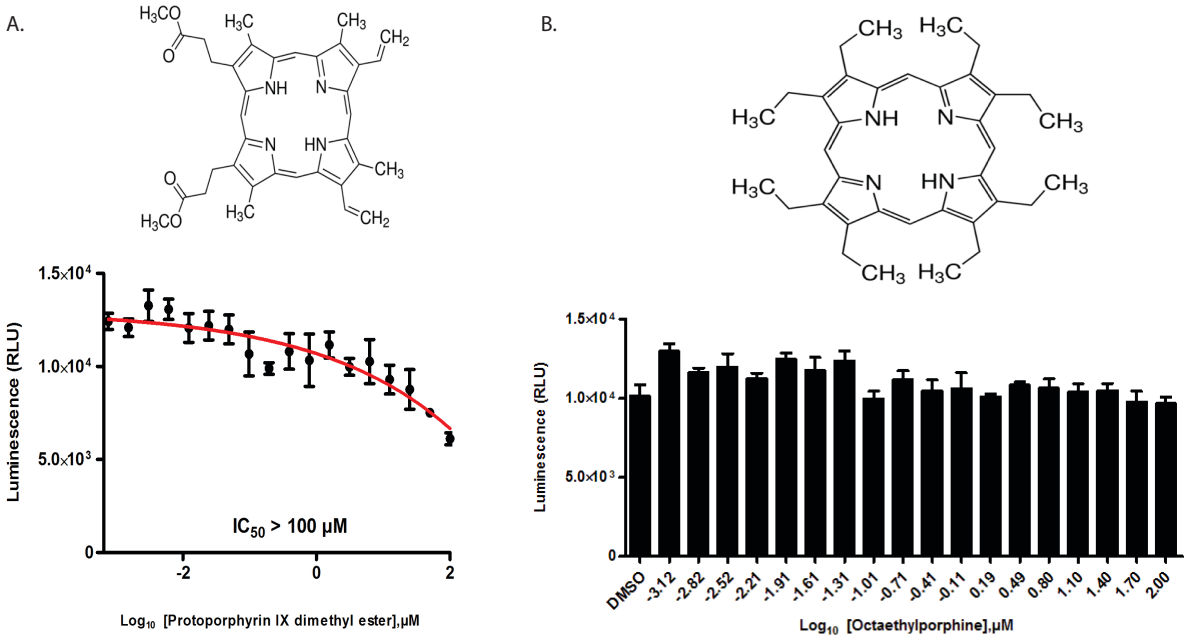

Figure S6. Verteporfin analogues with porphyrin rings do not inhibit OSR1 T185E in vitro. Two analogues of Verteporfin namely 2,3,7,8,12,13,17,18-Octaethyl-21H,23H-porphine (A) and protoporphyrin IX dimethyl ester (B) were used. The kinase assay was performed at 30 °C for 30 minutes by incubating 0.2 µM OSR1 T185E with increasing concentrations of Verteporfin in presence or absence of 5 molar excess of MO25 (1 µM) in a total assay volume of 5 µL. 250 µM CATCHtide, 0.1 mM ATP and 10 mM $MgCl_2$ were also used in the assay.

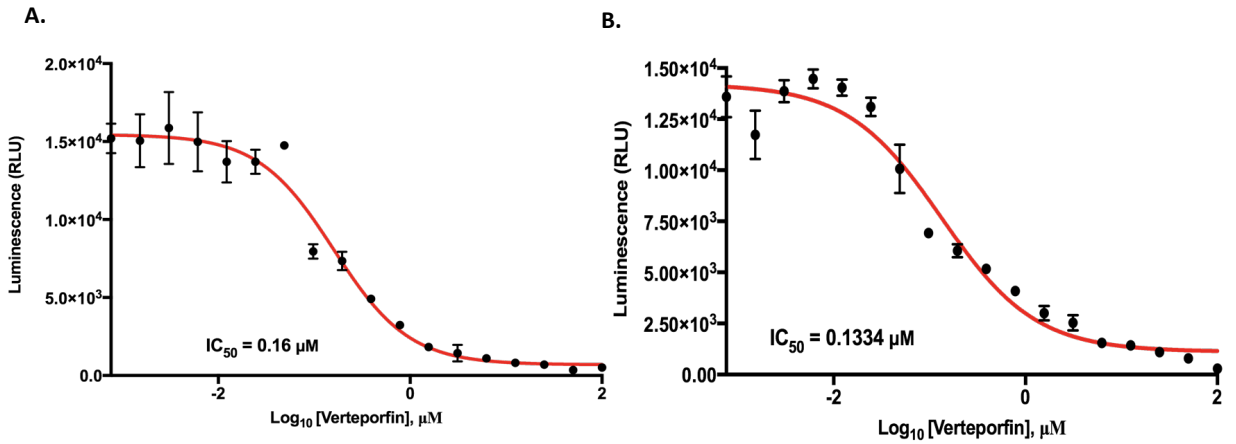

Figure S7. Verteporfin does not affect SPAK and OSR1 activation by MO25. The kinase assay was performed at 30 °C for 30 minutes by incubating 0.2 µM OSR1 T185E with increasing concentrations of Verteporfin in presence or absence of 5 molar excess of MO25 (1 µM) in a total assay volume of 5 µL. 250 µM CATCHtide, 0.1 mM ATP and 10 mM $MgCl_2$ were also used in the assay.

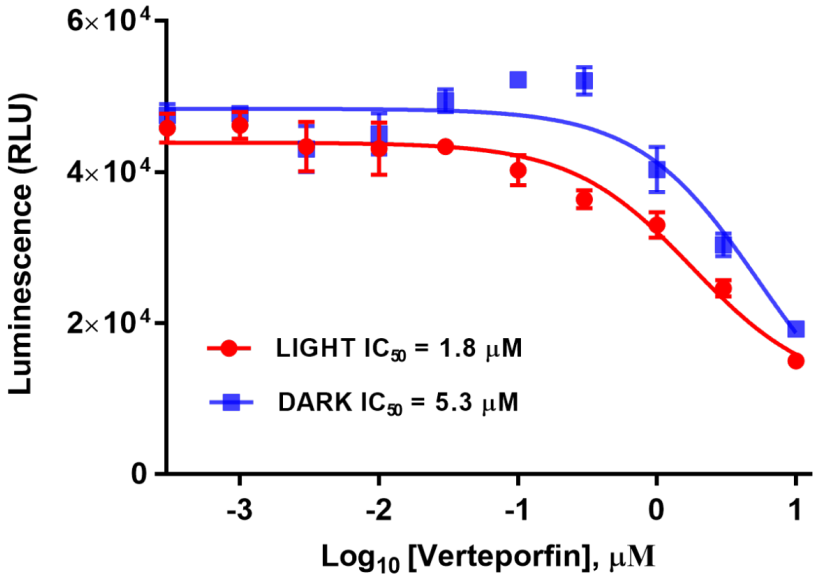

Figure S8. Light does not significantly affect Verteporfin's ability to inhibit OSR1 T18E in vitro. The kinase assay was performed at 30 °C for 30 minutes by incubating 0.2 µM OSR1 T185E with increasing concentrations of Verteporfin in a total assay volume of 5 µL. 5 µM recombinant human NKCC2 (1-174), 0.1 mM ATP and 10 mM $MgCl_2$ were also used in the assay. For dark assay conditions, the assay plate was covered in aluminum foil prior to the addition of Verteporfin and during the assay until the assay was finished the plate was being read.

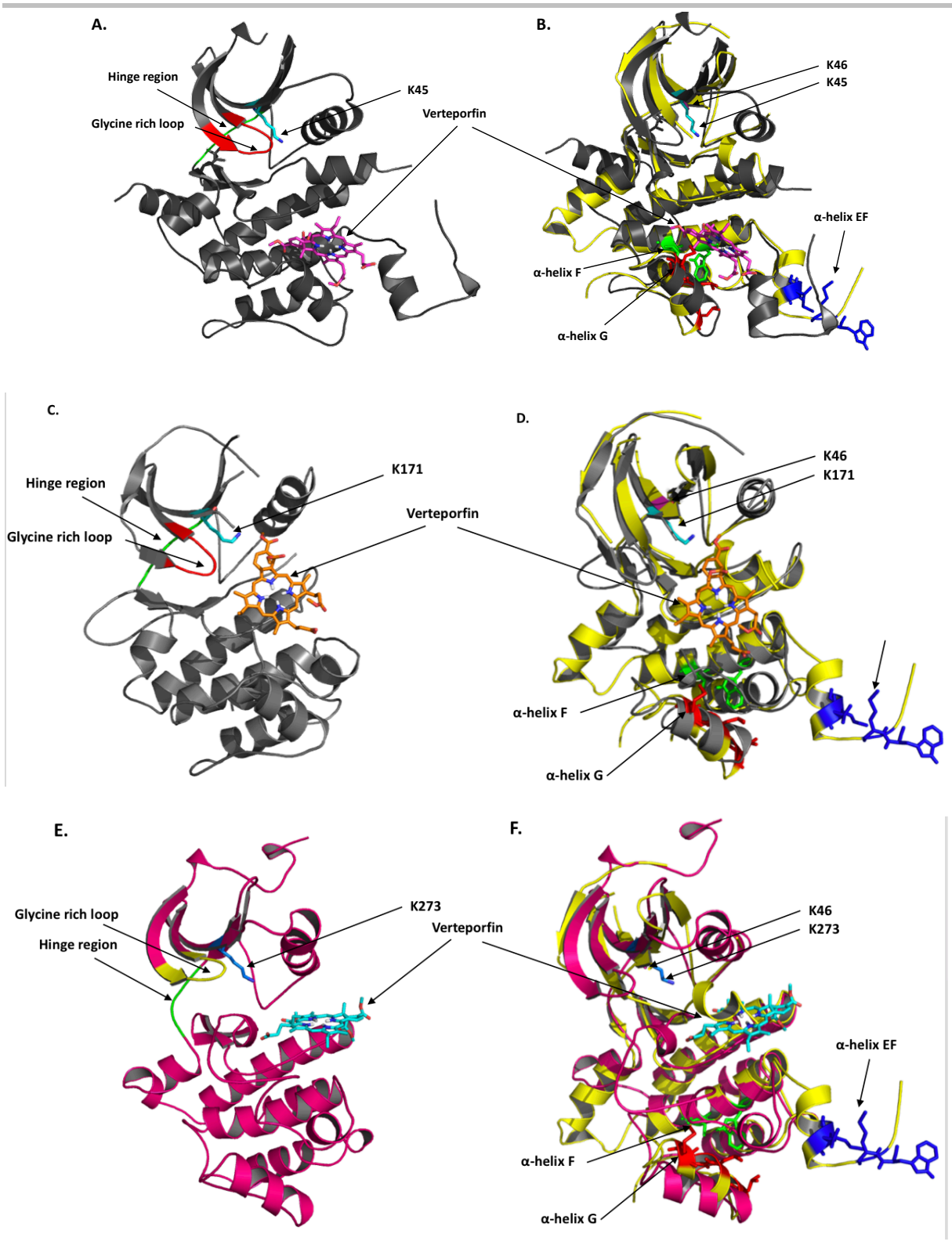

Figure S9. In Silico modelling indicates that Verteporfin does not bind the ATP pocket of hit protein kinases. A) Ribbon representation of Verteporfin (pink) bound to MAP4K3 (grey). B) Ribbon representation of structure alignment of the crystal structures of MAP4K3 kinase (PDB: 5J5T) (grey) and OSR1 kinase 1-303 (PDB: 2VWI) (yellow). Glycine rich loop and hinge region are shown in red and green color, respectively. Catalytic lysine of MAP4K3 (K45) and OSR1 (K46) are shown in cyan and pink sticks,

respectively. C) Ribbon representation of Verteporfin (orange) bound to MLK1 (grey). D) Ribbon representation of structure alignment of the crystal structures of MLK1 kinase (PDB: 3DTC) (grey) and OSR1 kinase 1-303 (PDB: 2VWI) (yellow). Glycine rich loop and hinge region are shown in red and green color, respectively. Catalytic lysine of MLK1 (K171) and OSR1 (K46) are shown in cyan and pink sticks, respectively. E) Ribbon representation of Verteporfin (cayan) bound to LCK (pink). F) Ribbon representation of structure alignment of the crystal structures of LCK kinase (PDB: 2PL0) (pink) and OSR1 kinase 1-303 (PDB: 2VWI) (yellow). Glycine rich loop and hinge region are shown in yellow and green color, respectively. Catalytic lysine of LCK (K273) and OSR1 (K46) are shown in blue and pink sticks, respectively. Similar results were found with MST2 and ULK1 in silico docking.